Plant Physiol. (1990) 94, 1024–1032
0032-0889/90/94/1024/09/$01.00/0

Received for publication April 9, 1990
Accepted June 21, 1990

Intercellular Diffusion Limits to CO_2 Uptake in Leaves[1]

Studies in Air and Helox

David F. Parkhurst* and Keith A. Mott

School of Public and Environmental Affairs and Biology Department, Indiana University, Bloomington, Indiana 47405 (D.F.P.), and Biology Department, Utah State University, Logan, Utah 84321 (K.A.M.)

ABSTRACT

We studied plants of five species with hypostomatous leaves, and six with amphistomatous leaves, to determine the extent to which gaseous diffusion of CO_2 among the mesophyll cells limits photosynthetic carbon assimilation. In helox (air with nitrogen replaced by helium), the diffusivities of CO_2 and water vapor are 2.3 times higher than in air. For fixed estimated CO_2 pressure at the evaporating surfaces of the leaf (p_i'), assimilation rates in helox ranged up to 27% higher than in air for the hypostomatous leaves, and up to 7% higher in the amphistomatous ones. Thus, intercellular diffusion must be considered as one of the processes limiting photosynthesis, especially for hypostomatous leaves. A corollary is that CO_2 pressure should not be treated as uniform through the mesophyll in many leaves. To analyze our helox data, we had to reformulate the usual gas-exchange equation used to estimate CO_2 pressure at the evaporating surfaces of the leaf; the new equation is applicable to any gas mixture for which the diffusivities of CO_2 and H_2O are known. Finally, we describe a diffusion-biochemistry model for CO_2 assimilation that demonstrates the plausibility of our experimental results.

Modelers and experimentalists studying carbon assimilation by plant leaves commonly assume that the partial pressure p_i (or concentration, c_i) of CO_2 is uniform throughout the intercellular air spaces in the leaf mesophyll (Table I provides a list of symbols and abbreviations used in this article). A corollary of this assumption is that CO_2 diffusion in the air spaces occurs with negligible 'resistance,' and presents negligible limitation to CO_2 assimilation. This article provides experimental evidence that internal air-space diffusion can substantially limit assimilation in some leaves, especially hypostomatous ones. This implies that p_i varies considerably with distance from the stomata in such leaves.

The assumption of uniform p_i has not always been made; early resistance-based models (*e.g.* 6, 7) sometimes included terms for an 'intercellular-diffusion-resistance' component. More recently, Bykov and Levin (1), Parkhurst (13, 15, 16), Rand (19), Rand and Cooke (20), and Gutschick (5) have described models that include intercellular diffusion explicitly, using differential equations for mass diffusion in place of questionable resistance analogies. These models predict differences of up to 10 Pa in CO_2 pressure from the substomatal cavity to the adaxial surface of hypostomatous leaves under some conditions. Parkhurst *et al.* (17) measured gradients similar to those predicted by the models, in amphistomatous ('amphi') leaves that simulated hypostomatous ('hypo') leaves because they were fed CO_2 from only one surface.

In addition to calculating CO_2 gradients in leaves, Parkhurst (16) used his 1986 model to estimate that carbon assimilation would increase by 24% in *Arbutus menziesii* if the diffusion coefficient in the intercellular air spaces of its thick, sclerophyllous leaves were increased, hypothetically, by a factor of one million. (This change can be interpreted as effectively eliminating any internal diffusion limitation, or 'resistance.' For a given process or pathway to be completely nonlimiting, its related 'conductance' must be essentially infinite.) This result suggests quite directly that intercellular diffusion limits photosynthetic carbon assimilation to an important extent in at least some leaves.

After hearing of this result, John R. Evans (personal communication, 1986) suggested that the calculations could be tested experimentally by measuring CO_2 assimilation in leaves placed in a helium-oxygen atmosphere instead of normal air. We report here the results of experiments based on that suggestion. The experiments work because CO_2 diffuses more rapidly through the smaller He atoms than through the larger N_2 molecules. (The diffusivity of CO_2 is about 3.6 times greater in pure He than in pure N_2—see "Appendix 2;" the presence of 21% O_2 reduces the difference to a factor of about 2.3, but even so, the effect is large enough to provide much useful information.)

We also describe a model that shows our results to be theoretically reasonable.

MATERIALS AND METHODS

Plant Material

Plants were grown in either controlled-environment greenhouses or controlled-environment growth chambers; they were watered and fertilized as necessary. For this initial survey, we studied one leaf of each of six amphi plants, and of seven hypo plants. We determined these categories by direct microscopic examination. The amphi plants were cocklebur (*Xanthium strumarium* L.), broad bean (*Vicia faba* L.), maize (*Zea mays* L.), ragweed (*Ambrosia cordifolia* Gray [Payne]) grown

[1] K.A.M. was supported by National Science Foundation grant No. DCB-8515578, and D.F.P. by the Indiana University School of Public and Environmental Affairs.

Table I. *Symbols and Abbreviations*

The following symbols are used throughout the text and are defined here.

Symbol	Abbreviation
a, c, h, w	Mole fractions (unitless) of air, CO_2, helox, and water vapor, respectively. Subscript a denotes ambient mole fraction in the leaf chamber; subscript i denotes the mole fraction at the evaporating surfaces of the leaf
$\bar{a}$, $\bar{c}$, $\bar{h}$, $\bar{w}$	$\bar{a} = (a_a + a_i)/2$, with similar definitions for the other gases
g_{ij}^k	A conductance [from Eq. [B11] of von Caemmerer and Farquhar (24)]. Subscripts (ij) denote conductances for gas j through gas i, with $i = a$ *or* h, and $j = c$ or w as defined above. Superscripts (k) are b, boundary layer; s, stomatal; and t, total. O_2 is oxygen; He is helium. Units assumed here are μmol m^{-2} s^{-1}
g_{liq}	Volumetric liquid-phase conductance from cell wall to chloroplast (μmol m^{-3} s^{-1} Pa^{-1})
g_s	Stomatal conductance (μmol m^{-2} s^{-1})
p	Local CO_2 partial pressure at a point in the intercellular air space of the mesophyll (Pa)
p_a	Ambient CO_2 partial pressure in the chamber surrounding the leaf (Pa)
p_i	CO_2 partial pressure at the evaporating surfaces in the leaf mesophyll, as determined by gas exchange measurements (Pa)
q	Local CO_2 partial pressure at the chloroplast (Pa)
r	Radial distance from the center of the stomatal pore (m)
w_{in}	Water vapor pressure entering chamber (kPa)
w_{out}	Water vapor pressure leaving chamber (kPa)
x, y	Cartesian coordinates in the plane of the leaf (m)
z	Cartesian coordinate perpendicular to the leaf surface (m)
A	Areal CO_2 assimilation rate (μmol m^{-2} s^{-1})
$\mathscr{A}$	Volumetric CO_2 assimilation rate (μmol m^{-3} s^{-1})
D_{ij}	Diffusivity of gas j through gas i; see g_{ij}^k (m^2 s^{-1})
E	Water-vapor flux density (μmol m^{-2} s^{-1})
K_a	Michaelis-Menten constant for activation of ribulose-1,5-bisphosphate carboxylase/oxygenase (hereafter referred to in this table as Rubisco) by CO_2 (Pa)
K_m	Effective Michaelis-Menten constant for CO_2, accounting for competitive inhibition by O_2 (Pa)
T	Filter paper temperature (°C)
V_c	Local volumetric carboxylation rate (μmol m^{-3} s^{-1})
$V_{c,max}$	Local maximum volumetric carboxylation rate when Rubisco is fully activated and when CO_2 and RuP_2 are not limiting (μmol m^{-3} s^{-1})
V_j	Local volumetric potential carboxylation rate as limited by electron transport and photophosphorylation (μmol m^{-3} s^{-1})
W_c	Local volumetric Rubisco-limited carboxylation rate (μmol m^{-3} s^{-1})
W_j	Local volumetric carboxylation rate as limited by RuP_2 regeneration (μmol m^{-3} s^{-1})
α	Smoothing factor for the transition between Rubisco limitation and RuP_2 limitation (μmol m^{-3} s^{-1})
β	Factor to match units between the diffusion rate to a point and the assimilation rate at that point (m^3 Pa μmol^{-1})
ϕ_i, ϕ_j, ϕ_k	Local values of porosity (air-space fraction) over tortuosity in the x, y, and z directions, respectively (unitless)
Γ_*	CO_2 compensation point (Pa)
amphi	Amphistomatous
hypo	Hypostomatous
air	79:21 nitrogen:oxygen mixture, with varying added amounts of H_2O and CO_2
helox	79:21 helium:oxygen mixture, with varying added amounts of H_2O and CO_2

in full sun, Chinese hibiscus (*Hibiscus rosa-cinensis* L.), and soybean (*Glycine max* Merr.). The hypo plants were grape ivy (*Cissus rhombifolia* Vahl); oleander (*Nerium oleander* L.); three plants of ragweed grown in full sun, partial sun, and shade; Schefflera (*Brassaia actinophylla* Endl.); and Swedish ivy (*Plectranthus australis* R.Br.). *A. cordifolia* is interesting because it generally produces amphi leaves when grown in full sun, and hypo leaves when grown in lower light (12); we have used both types here. Plants varied in age from a few weeks in broad bean to a few years in hibiscus. All leaves were fully expanded, but not senescing.

Gas Exchange

Separate gas-mixing systems were used to combine nitrogen or helium with oxygen, CO_2, and water vapor in the chosen proportions. Both systems used metering valves to mix nitrogen and oxygen ('air,' but without minor components other than water and CO_2) or helium and oxygen ('helox') in 79:21 ratios (v/v). In each system a portion of this mixture was then humidified by bubbling it through heated, deionized water that had been pre-equilibrated with CO_2-free helox or air. The humidified mixture then passed through a temperature-controlled condenser to produce a known water-vapor pressure, and was remixed with the dry gas. The flow rates of the 'dry' and 'wet' gases were regulated using electronic mass-flow controllers. To keep the total flow of gas through the system approximately constant, the sum of the dry and wet flows was kept constant. After humidification, 1% CO_2 in helox or air was added to the CO_2-free helox or air mixtures with a mass-flow controller. By varying the settings of the three mass-flow controllers, we could rapidly and reliably control the partial pressures of CO_2 and water vapor in the gas entering the chamber.

Mass-flow meters and controllers used with helox were calibrated with helox. Band-broadening in both helox and air was measured and corrected for. Measurement was accomplished by drying (with $MgClO_2$) one-half of a gas stream of known CO_2 and water-vapor concentration. The two halves of the gas stream were then passed through the reference and analytical cells of the differential analyzer. The difference in CO_2 concentration between the cells was corrected for dilution by water vapor, and the remaining difference was attributed to band-broadening. The magnitude of the difference varied linearly with the difference in water-vapor concentration between the two cells of the analyzer. It was independent of the absolute water-vapor concentration but linearly dependent on the absolute CO_2 concentration.

A portion of the final mixture passed through an absolute CO_2 infrared gas analyzer (ADC, Mk III), and another portion through a chilled-mirror dewpoint hygrometer (General Eastern, DEW-10), to allow determination of the CO_2 and water vapor partial pressure of the gas after mixing. A third portion of the mixture passed through the reference cell of a differential CO_2 infrared gas analyzer. The remainder of the mixture passed through a mass-flow meter and then to the leaf chamber. A sample of the gas exiting the leaf chamber was picked up at positive pressure and pumped through a dewpoint hygrometer and the analysis cell of the differential CO_2 analyzer.

The leaf chamber, constructed of nickel-plated aluminum, contained two miniature fans that circulated air through a heat exchanger and past the leaf. The temperature of the heat exchanger was controlled with a water bath. Leaf temperature was determined with a fine-wire (0.27 mm diameter), chromel-constantan thermocouple. Irradiance was measured with a small gallium-arsenide photodiode mounted inside the chamber adjacent to the leaf. This sensor was calibrated with a Li-Cor quantum sensor under the metal-halide lamp used to illuminate the leaf in the chamber. Irradiance ranged from 800 to 900 $\mu E\ m^{-2}\ s^{-1}$; these levels were likely saturating for all the plants, except perhaps the maize.

The electronic outputs of the various system components were monitored with a portable data logger (Campbell Scientific, 21x) interfaced with a microcomputer to provide real-time calculations of gas-exchange parameters. Gas-exchange parameters in air were calculated using the equations given by von Caemmerer and Farquhar (24). For helox, their equations had to be modified as outlined in "Appendix 1."

Diffusion Ratios for Helox and Air

To show that we could match the known diffusion ratio for water vapor in helox and air in our system, we constructed an artificial leaf from a porous plate. Twenty-five holes of 1.6 mm diameter were drilled in a 6.45-cm^2 aluminum plate that was approximately 3 mm thick. Filter paper was sealed between this plate and an aluminum-foil base, and a wick of filter paper sealed with aluminum foil was used as a 'petiole.' To prevent turbulence inside the pores of the diffusion plate, the top of the plate was covered with nylon mesh with 30-μm pores. The entire assembly was placed in the chamber in place of a leaf, with the filter-paper wick extending out into a beaker of distilled water. The diffusional conductance of this artificial leaf was determined in both helox and air, with transpiration rate, E, held constant by adjustments made to the vapor pressure of the gas mixture entering the chamber. Then the ratio of conductances was calculated for comparison with the known diffusivity ratio. In both this and the following checks, boundary-layer conductances were scaled by the two-thirds power of diffusivity, in the usual way (24).

As a second check of the water-vapor diffusion ratio, we held a hypo, shade-grown ragweed leaf in air until its transpiration rate remained constant, and then averaged the corresponding stomatal conductance over a 4-min period. Then we switched to helox, and allowed the transpiration rate to come to a new, higher, steady rate. Finally, we switched back to air to show that the initial rate had not changed (which would have indicated a change in stomatal aperture). We then calculated the ratio of the stomatal conductances to water vapor in the two gas mixtures. These measurements were similar to those of Egorov and Karpushkin (2).

Assimilation *versus* p_i Curves

The rate of photosynthetic CO_2 assimilation was determined as a function of p_i in helox and air by first allowing the leaf to reach steady state in air at 29 Pa CO_2 (340 μL/L at 86 kPa atmospheric pressure in Logan, UT) and 1.5 kPa H_2O. Helox was then substituted for air, with partial pressures

of CO_2 and H_2O adjusted to maintain p_i and transpiration rate approximately the same as for the previous point in air. Air was then reintroduced to the chamber at a different CO_2 partial pressure, and the process was repeated. Leaf temperature was maintained at 25.0 ± 0.1°C throughout the experiment.

DIFFUSION-RATIO CALIBRATION RESULTS

Table II shows the results of the porous-plate measurements. The ratio of diffusion rates through the plate in the two gas mixtures, 2.28, compared well with the 2.33 ratio of diffusivities presented in Table IV.

Figure 1 shows the stomatal conductances for the ragweed leaf in the two gas mixtures. The ratio of these conductances (helox:air) was 2.1 (0.839:0.406), which is close to, but slightly smaller than, the theoretical value. One explanation for the difference may be that some Knudsen diffusion takes place in the stomatal pore (2, 9). Alternatively, the lower-than-expected transpiration rate in helox may indicate that under the nearly doubled evaporation rate in the helox, the water evaporated from cell walls that were further into the mesophyll from the substomatal cavity, thereby decreasing the overall conductance to water vapor relative to that in air.

RESULTS OF CO_2 EXCHANGE MEASUREMENTS

Figure 2 shows A-p_i curves for soybean, with amphi leaves, and for Schefflera, with hypo leaves. The curves are purely empirical cubic splines that we fit for purposes to be explained below.

Curves for other amphi leaves were generally similar to the soybean curves, with A (for given p_i) being similar for both host gases, but most often slightly higher in helox than in air. Curves for other hypo leaves were generally like those for Schefflera. Figures 3 and 4 show the data for all leaves in a different form, with the ratio of A in helox to A in air plotted against p_i. The points correspond to p_i values for which we have helox data; the A values for air at those points were interpolated from the cubic-spline curves, because we seldom had data for *exactly* the same p_i values in both media. Controlling CO_2 levels entering the chamber allowed us to maintain p_i in helox to within a few μL/L of its value in air, and the interpolation procedure then corrected for the remaining minor differences to allow direct comparisons of A values at fixed p_i values. The plotted ratios show how much greater assimilation was in helox than in air. Figure 3 shows that the helox:air assimilation ratios were greatest at low p_i, and lower as p_i increased. This is an important result for reasons to be discussed below.

Statistically, we note that 47 of 48 points for the hypostomatous leaves were greater than unity. For these points, $A_{helox} - A_{air}$ was positive, so we applied the sign test (25) and found that the probability of obtaining 47 or 48 positive values in 48 measurements, if a null hypothesis of no mean difference were true, would be $P = 1.74 \times 10^{-13}$. Clearly we can reject the no-difference hypothesis. For the amphistomatous leaves, 32 of 43 ratios were greater than unity. Here the sign test gives P = 0.001. Thus, although the intercellular diffusion limitation to assimilation was generally smaller in amphi than in hypo leaves, the limitation was statistically detectable even in the amphi leaves.

Table II. *Results of the Calibration with the Artificial Leaf*

Gas mixture	w_{in}[a] (kPa)	w_{out} (kPa)	T (°C)	g_s (μmol m^{-2} s^{-1})	E (μmol m^{-2} s^{-1})
Air	0.0839	0.0962	25.06	2.23×10^5	5.13×10^3
Helox	2.064	2.155	25.03	5.08×10^5	5.09×10^3
			Ratio	2.28	

[a] w_{in}, water vapor pressure entering chamber; w_{out}, water vapor pressure leaving chamber; T, filter paper temperature; g_s, 'stomatal' conductance; E, water-vapor flux density.

MODEL DEVELOPMENT

To show that these results are theoretically feasible, we used a modification of the model described by Kirschbaum and Farquhar (8), as developed by D. F. Parkhurst, G. D. Farquhar, and I. R. Cowan (unpublished). The Kirschbaum-Farquhar (8) model treats the biochemistry of carbon assimilation on an average basis throughout the mesophyll, and expresses the results, $\mathscr{A}$, on an areal basis in μmol CO_2 per m^2 of adaxial surface per s.

The modification allows for p to vary throughout the mesophyll, rather than remaining constant at the measured p_i value. It assumes the Kirschbaum-Farquhar (8) model to hold for the *local* volumetric assimilation $\mathscr{A}$ in μmol per m^3 of mesophyll tissue per s, as a function of the *local* CO_2 partial pressure at the chloroplasts. Then, it equates that local uptake to the net diffusion to the point. The result is the following series of equations:

$$D_{ic}\left[\frac{\partial}{\partial x}\left(\phi_i \frac{\partial p}{\partial x}\right) + \frac{\partial}{\partial y}\left(\phi_j \frac{\partial p}{\partial y}\right) + \frac{\partial}{\partial z}\left(\phi_k \frac{\partial p}{\partial z}\right)\right] = \beta\mathscr{A}(q) \quad (1)$$

$$\mathscr{A}(q) = V_c\,(1 - \Gamma_*/q) \quad (2)$$

$$V_c = sr[V_c^2 - V_c\,(W_c + W_j + \alpha) + W_c W_j] \quad (3)$$

$$W_c = \left(\frac{q}{q + K_a}\right)\left(\frac{q}{q + K_m}\right) V_{c,max} \quad (4)$$

$$W_j = \frac{V_j}{\left(1 + \frac{7\Gamma_*}{3q}\right)} \quad (5)$$

Equation 1 is modified from Parkhurst (13, 15), and Equations 2 to 5 are from Kirschbaum and Farquhar (8). In Equation 3, 'sr' denotes the smaller of the two roots of the quadratic equation indicated. Equation 1 involves the gas-phase CO_2 pressure, p, on the left-hand side, and the liquid-phase pressure, q, on the right. We couple these with the relation:

$$\mathscr{A} = g_{liq}(p - q) \quad (6)$$

which models the liquid phase diffusion from the outer cell wall into the chloroplast. Ian Cowan (personal communication, 1985), based on work by Evans (3, 4), has estimated g_{liq} to be approximately 0.5 μmol m^{-2} (of chloroplast area) s^{-1} Pa^{-1}, and we use that value here.

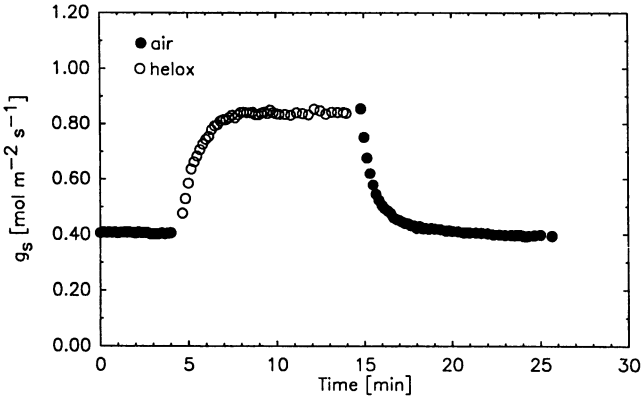

Figure 1. Time course of stomatal conductance of a hypostomatous ragweed leaf, as the gas mixture was changed from air to helox and back to air.

The model represented by these equations is related to those of Rand (19), Rand and Cooke (20), and Gutschick (5). However, it differs from the latter models in treating intercellular diffusion as the three-dimensional process that it really is (13, 15). The present model also incorporates more sophisticated descriptions of the biochemical processes of carbon assimilation, as developed by Farquhar and his colleagues (*e.g.* 8).

The partial differential Equation 1, with its associated relationships (Eqs. 2–6), can only be solved in terms of a particular geometry, and with particular boundary conditions. Parkhurst (15) has described the solution of a version of this model having simpler biochemistry, but assuming that each stoma supplies CO_2 to a cylindrical region of tissue with the stoma on one face of the cylinder. For present purposes, we have approximated the leaf's geometry by assuming that each stoma provides CO_2 to a hemispherical region of tissue, as detailed in "Appendix 2."

The assumption of a hemispherical 'territory' for each

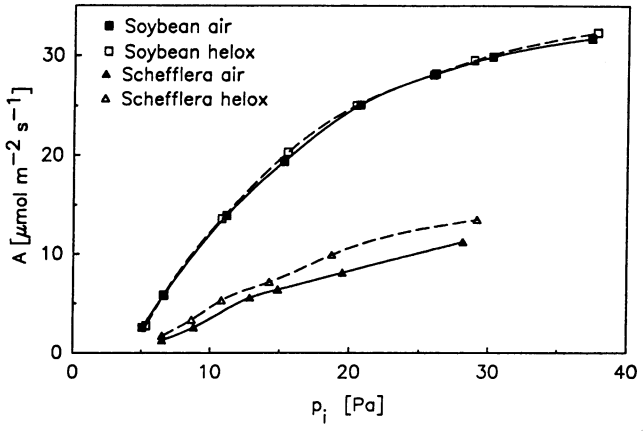

Figure 2. Measured A-p_i relationships for soybean, with amphistomatous leaves, and for Schefflera, with hypostomatous leaves, in air and in helox. Curves are cubic splines fit to the data to allow interpolation. For both plants, the open symbols represent the A-p_i relationship in helox, and the closed symbols the relationship in normal air.

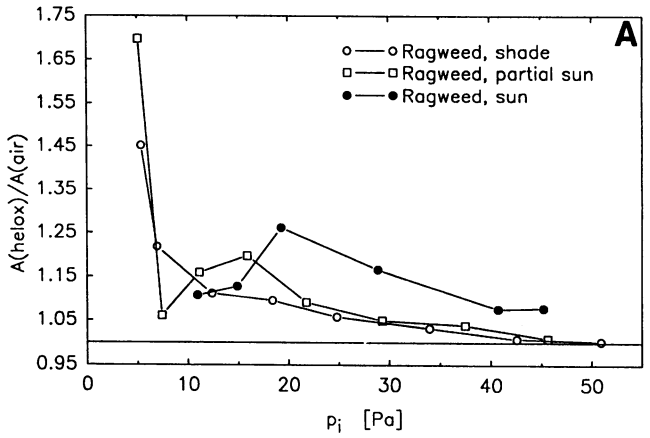

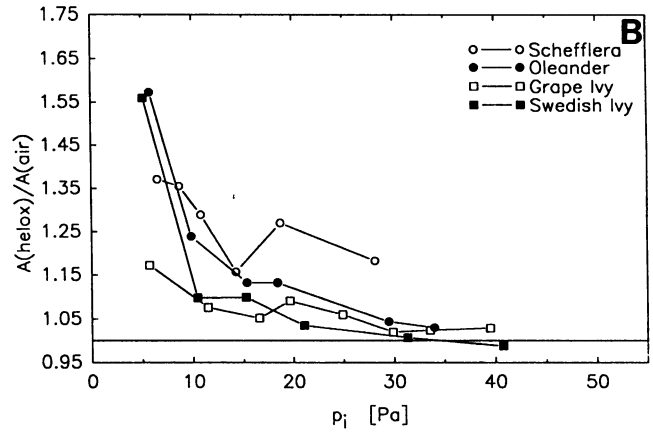

Figure 3. Ratios of whole-leaf CO_2 assimilation (A) in helox to assimilation in air, with p_i held constant, for leaves of seven hypostomatous plants. A, ragweed, grown in sun, partial sun, and shade; B, other species.

stoma deals with the fact that in a real, three-dimensional leaf (*cf.* ref. 15), there is a greater volume of tissue in the region that is 40 to 50 μm from the stoma (for example) than in the region that is 30 to 40 μm from the stoma. Hemispherical geometry somewhat exaggerates the average distance from stoma to various points on chlorenchyma cell wall, relative to the average distance in a cylindrical 'territory.' However, this helps to correct for the greater photosynthetic potential of the cells near the upper, sunlit surface of leaves (22, 23). In any case, the model is used here as a general plausibility argument for our measured results, rather than to provide exact quantitative predictions.

MODEL RESULTS

We solved the above model as described in "Appendix 2," first assuming the intercellular air spaces of the mesophyll to be filled with air, and then with helox. The two nearly parallel curves (Fig. 5) then show the calculated leaf assimilation rates for a hypo leaf with a mesophyll 350 μm thick, and having biochemical properties similar to those given by Kirschbaum and Farquhar (8) for *Eucalyptus pauciflora*. These curves are similar in general form to those for Schefflera in Figure 2, with higher A values in helox than in air. The ratio of A in

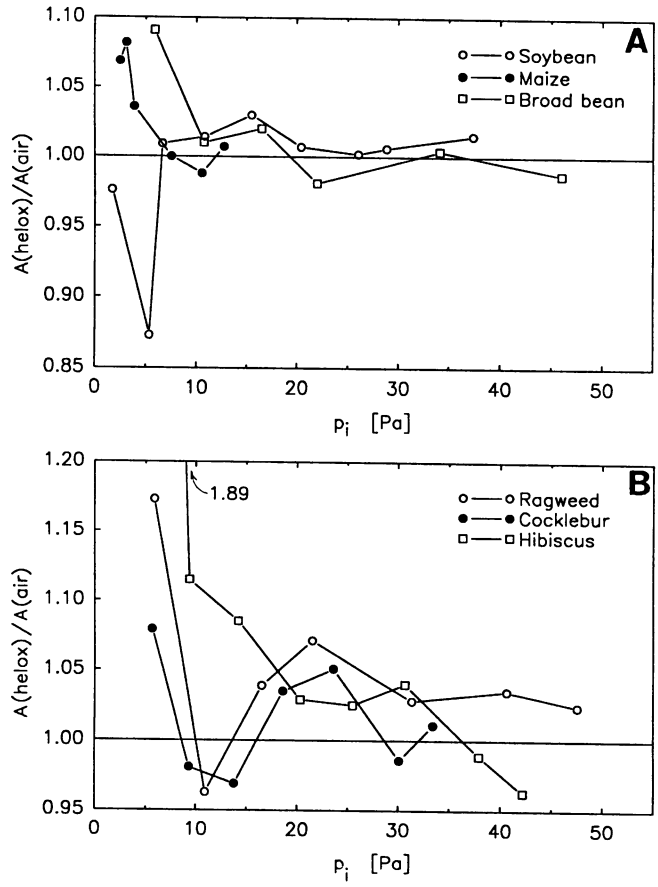

Figure 4. Ratios of whole-leaf CO_2 assimilation (A) in helox to assimilation in air, with p_i held constant, for leaves of six amphistomatous plants. A, three common agricultural species; B, three other species.

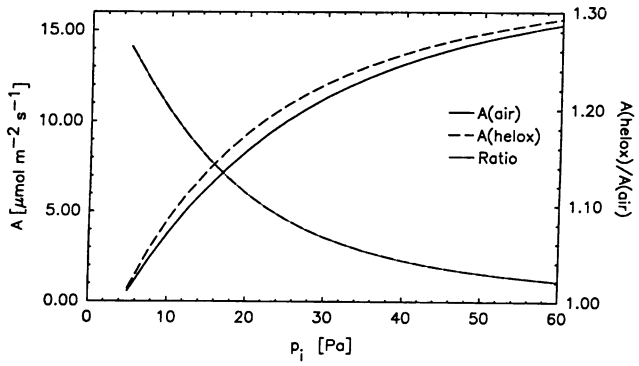

Figure 5. Model results, showing A *versus* p_i for a hypothetical leaf in air and helox (left axis), and the ratio of A in helox to A in air (right axis).

Table III. *Relative Increases in Leaf Assimilation of CO_2 in Helox Compared with Air, in Leaves Exposed to Ambient Partial Pressures of CO_2 of p_a = 29 Pa When in Air*

Corresponding p_i values (matched in air and helox) are also listed.

Plant	p_i	A_{helox}:A_{air}[a] [Ratio has no units.]
Hypostomatous leaves:		
Ragweed (sun)	21.1	1.27
Schefflera	ND[b]	1.17
Oleander	19.4	1.13
Grape ivy	19.1	1.09
Ragweed (partial sun)	21.5	1.09
Ragweed (shade)	24.8	1.06
Swedish ivy	21.5	1.03
Geometric mean (hypo leaves)		1.12
Amphistomatous leaves:		
Ragweed (sun)	21.8	1.07
Hibiscus	19.9	1.03
Cocklebur	18.5	1.03
Soybean	20.7	1.01
Maize	10.3	0.99
Broad bean	22.2	0.98
Geometric mean (amphi leaves)		1.02

[a] A_{helox}, areal CO_2 assimilation rate in helox; A_{air}, areal CO_2 assimilation rate in air. [b] Not determined.

helox to A in air is also shown in Figure 5, with the scale for this ratio on the right-hand vertical axis. This curve is quite similar in form to the A-ratio curves for our measurements with hypo leaves (Fig. 3).

DISCUSSION AND CONCLUSIONS

We begin by noting an important assumption that underlies the interpretation of our results, *i.e.* that helium affects CO_2 assimilation only by modifying gaseous diffusion rates. However, we know of no evidence that this inert gas would have any other effects on leaves. Further, because changes in assimilation rates are rapidly reversible when the leaf is returned to air, it is clear that helium causes no permanent changes (at least) in the leaf's normal function. Also, the major differences in the effect of helox between hypo and amphi leaves are consistent with a gaseous-diffusion effect, and would not be consistent with any other kind of effect that we can imagine.

For leaves to assimilate CO_2, the gas must first diffuse through the external boundary layer and then through a stoma into a sub-stomatal chamber. From there, it must diffuse as a gas through the intercellular air spaces until it reaches a mesophyll cell wall. There it dissolves in the water on the cell wall, and then diffuses in the liquid phase (either as CO_2 or bicarbonate) until it reaches a chloroplast where the actual carbon assimilation takes place.

In this series of processes, the intercellular diffusion can only take place down CO_2 gradients. Thus, the CO_2 pressure must be lower at the mesophyll cell walls than it is in the substomatal cavity, for any cells having positive net assimilation. As a result, photosynthesis must be lower than it would be if

CO_2 pressure at all cell walls were as high as that in the substomatal cavity, whenever CO_2 is at least partially limiting at the chloroplast level. Finally, then, intercellular diffusion of CO_2 must limit assimilation to some extent whenever this latter condition holds. The question is, how limiting?

By replacing nitrogen (mol wt 28) with helium (atomic weight 4) in our leaf chamber, we have reduced the diffusion limitation to about 43% of its usual value. When we switched from air containing 340 μL/L CO_2 to helox, and adjusted p_a so as to hold p_i constant, net assimilation increased by 3 to 37% in the hypostomatous leaves we studied (Table III). The average increase under these conditions was 12%. The averages listed are geometric means (antilogs of mean logarithms; see ref. 25), which are more appropriate than arithmetic means for ratios. At lower ambient CO_2 levels, the increases of A in helox were even greater (Fig. 3).

For amphistomatous leaves, in which diffusion distances are only about half what they would be in hypo leaves of equal thickness, the assimilation increase in helox ranged from −2 to +7%, and averaged about +2% (Table III; Fig. 4). The negative values (corresponding to ratios less than unity) may indicate small measurement errors caused by our gas-exchange equipment, or they may have resulted from normal temporal changes in leaf response as we switched from air to helox. Another possibility is that, because leaf evaporation rates were sometimes higher in helox than in air, photosynthesis might have been reduced somewhat by a tissue-drying effect. Stomatal effects should not be involved, however, because we are comparing A values for the two gas mixtures with p_i held constant.

Because the diffusivity of CO_2 in helox is not infinite, we have not completely eliminated the intercellular, gaseous-diffusion limitation to whole-leaf CO_2 assimilation, even in helox. The true diffusive limitations must be even greater than the reductions we have achieved here. One can obtain a rough estimate of the total intercellular diffusion limitation by assuming that CO_2 assimilation is approximately a linear function of the reciprocal of CO_2 diffusivity. Now, let relative assimilation be 1.0 in air (with $1/D_{ac} = 1/0.188 = 5.32$ s cm^{-2}), and 1.02 in helox (with $1/D_{hc} = 1/0.438 = 2.28$ s cm^{-2}). Then, intercellular diffusion would be completely nonlimiting only when $1/D_{ic} = 0$, for which value relative assimilation would be 1.035. This suggests that intercellular diffusion accounts for about 3.5% of the total assimilation limitation on average in the amphi leaves that we studied. The intercellular limitation corresponding to the average 12% increase in A that we measured in hypo leaves would be a substantial 21%.

Note that with both hypo and amphi leaves (Figs. 2–4), the relative increase of A in helox to that in air is greatest at low p_i. This is consistent with the fact that the A-p_i curve is steepest at low p_i, and flatter at high p_i. Put another way, as CO_2 becomes plentiful at the chloroplasts, enzymatic activity becomes limiting, so increasing the CO_2 supply has less effect on increasing assimilation. Leaves with relatively steep A-p_i curves at normal external CO_2 levels would benefit more in nature from a reduced gaseous-diffusion limitation than would leaves with lower A-p_i slopes. Thus the former sort of leaf would likely benefit more from amphistomy (compared with hypostomy) than would the latter sort.

We have shown, then, that intercellular CO_2 diffusion can limit CO_2 uptake to an important extent, especially in hypostomatous leaves, but even by as much as 7% (at normal CO_2 levels) in amphistomatous leaves of ragweed. One reviewer asked that we indicate at what p_i levels intercellular diffusion may be limiting. The answer is that complex processes like carbon assimilation are seldom limited by a single factor at any one time. Thus, intercellular diffusion will be at least partially limiting at any p_i level where the slope (dA/dp_i) of the A-p_i curve is greater than zero. As discussed in the previous paragraph, the effect will be greatest at low p_i, but it will seldom be completely negligible.

The fact that intercellular CO_2 diffusion is sometimes an important limitation has four other consequences. The first is that this limitation implies the existence of substantial CO_2 pressure gradients within normally operating leaves; this corroborates the measurements made by Parkhurst *et al.* (17) with amphi leaves used to simulate hypo ones. Thus, photosynthesis models that assume p_i to be equal throughout the mesophyll to the value estimated by normal gas-exchange measurements will be based on an overestimate of the true assimilation-weighted average CO_2 pressure within the mesophyll.

A second consequence is that attempts to partition limitations to assimilation to various causes will be incorrect to the extent that this cause is neglected. That is, if the intercellular diffusion limitation is ignored in studies of leaves where it is important, then its effects will be assigned incorrectly to other causes, such as *intra*cellular diffusion, or biochemistry. In such cases, the importance of the other limitations will be overestimated.

Third, the present results provide support for modeling efforts aimed at understanding the adaptive nature of internal leaf structure from the point of view of its effects on reducing the diffusive limitation (15). Indeed, Parkhurst (14) used such arguments to predict that amphistomy would increase CO_2 assimilation rates relative to hypostomy, and our present results are consistent with that prediction. From another point of view, the fact that the helox effect was generally greater in hypo than in amphi leaves is evidence that intercellular diffusion, rather than some other cause, is the explanation for our results.

Fourth, given the smaller diffusive limitations that exist in amphistomatous leaves, we remain hard put to explain why so many plants in nature have hypo leaves (*cf.* 12, 14).

We note the usefulness of helox for gas exchange studies. Animal physiologists have used it for many years (*e.g.* 21), and Egorov and Karpushkin (2) used it to study water loss from leaves. Helox is difficult to work with because the small helium atoms 'leak' easily through any cracks and pores in a system. But used with care it has great potential for other leaf studies; it might be used, for example, to investigate how deeply in the mesophyll pollutant gases like SO_2 and ozone are taken up.

APPENDIX 1

Modifying the von Caemmerer-Farquhar Equations for Use with Helox and Other Host Gases

In deriving their widely used gas-exchange equations, von Caemmerer and Farquhar (24; hereafter vC & F) made use of

the convenient fact that the molecular diffusivity of CO_2 through air is numerically nearly equal to its diffusivity through water vapor (*i.e.* $D_{ac} \approx D_{wc}$). This allowed them to simplify their equation [B10]:

$$(c_i - c_a) = -\left(\frac{\bar{a}}{g^t_{ac}} + \frac{\bar{w}}{g^t_{wc}}\right)A - \frac{\bar{c}E}{g^t_{wc}} \tag{7}$$

to their equation [B17]:

$$A = gg^t_{ac}(c_a - c_i) - \bar{c}E. \tag{8}$$

This simplification does not hold for gas-exchange experiments in helox, however, because g^t_{hc} is quite different from g^t_{wc}.

As a result, the equation for c_i (the mole fraction of CO_2 at the evaporating surfaces of the leaf) becomes more complex for helox than the vC & F equation [B18] for air. We derive the c_i equation for helox here; the new form will apply to *any* host-gas mixture, including air, pure helium, or xenon-oxygen for example.

We first substitute $\bar{c} = (c_i + c_a)/2$ into the last term of Equation 7, and solve for c_i:

$$c_i = \frac{c_a - \left(\frac{c_a}{2g^t_{wc}}\right)E - \left(\frac{\bar{h}}{g^t_{hc}} + \frac{\bar{w}}{g^t_{wc}}\right)A}{1 + \frac{E}{2g^t_{wc}}} \tag{9}$$

where we have replaced g^t_{ac} with g^t_{wc}. However, $\bar{h} = 1 - \bar{w} - (c_i + c_a)/2$, so we substitute that expression and solve once again for c_i to obtain:

$$c_i = \frac{c_a - \left(\frac{c_a}{2g^t_{wc}}\right)E + \left[\frac{1}{g^t_{hc}}\left(\frac{c_a}{2} - 1\right) + \bar{w}\left(\frac{1}{g^t_{hc}} - \frac{1}{g^t_{wc}}\right)\right]A}{1 + \left(\frac{1}{2g^t_{wc}}\right)E - \left(\frac{1}{2g^t_{hc}}\right)A}. \tag{10}$$

To use this equation to estimate c_i, one must estimate the various conductances, g^k_{ij}. For this purpose, the equivalent of the vC & F equations [B14] to [B16] hold in helox as well as in air. These are:

$$g^t_{hw} = \frac{E(1 - \bar{w})}{w_i - w_a} \tag{11}$$

$$\frac{1}{g^t_{hw}} = \frac{1}{g^s_{hw}} + \frac{1}{g^b_{hw}}, \tag{12}$$

and:

$$\frac{1}{g^t_{hc}} = \frac{1}{g^s_{hc}} + \frac{1}{g^b_{hc}}. \tag{13}$$

To make use of these, we must know the diffusivities of water vapor in helox (D_{hw}) and of CO_2 in helox (D_{hc}). For the present work (at 25°C), we used the values in Table IV. Diffusivities for mixtures like helox are obtained by inverse averaging (2). Thus, for helox (21% O_2, 79% He):

$$\frac{1}{D_{hc}} = \frac{0.21}{D_{O_2,c}} + \frac{0.79}{D_{He,c}}. \tag{14}$$

Table IV. *Molecular Diffusivities (in $cm^2\ s^{-1}$) for Water Vapor and CO_2 as Minor Components in Various Host Gases, at 25°C and 86 kPa Total Pressure*

Values for water vapor are from Egorov and Karpushkin (2), and values for CO_2 from Mason and Marrero (11).

Host Gas or Mixture	D_{iw} for H_2O	D_{ic} for CO_2	Ratio, H_2O:CO_2
H_2O	—	0.191	—
O_2	0.314	0.187	1.68
N_2	0.294	0.188	1.57
He	1.025	0.683	1.50
Air	0.298	0.188	1.59
Helox	0.695	0.438	1.59

Now:

$$g^s_{hc} = g^s_{hw}\left(\frac{D_{hc}}{D_{hw}}\right) \tag{15}$$

and:

$$g^b_{hc} = g^b_{hw}\left(\frac{D_{hc}}{D_{hw}}\right)^{2/3} \tag{16}$$

as described in vC & F. With these relationships, c_i can be calculated from the usual gas-exchange measurements.

Finally, note from Table IV that:

$$\frac{D_{hc}}{D_{ac}} = \frac{D_{hw}}{D_{aw}} = 2.33.$$

APPENDIX 2

Details of the Diffusion-Uptake Model

For purposes of this article, we developed a version of the model represented by Equations 1 to 6 that could be more easily solved but that still incorporates the major features of the real situation. To do this, we changed Equation 1 into an ordinary differential equation representing diffusion from a small sub-stomatal cavity into a hemispherical region surrounding it:

$$\phi D_{ic}\frac{d}{dr}\left(r^2\frac{dp}{dr}\right) = r^2\beta\left[V_c\left(1 - \frac{\Gamma_*}{q}\right)\right]. \tag{17}$$

This is a better simplification than its analog in rectangular coordinates,

$$\phi D_{ic}\frac{d^2p}{dr^2} = \beta\left[V_c\left(1 - \frac{\Gamma_*}{q}\right)\right], \tag{18}$$

because the latter effectively "smears" the stomatal conductance evenly over the whole leaf surface and neglects the nearly point-source nature of real stomata (15).

To obtain the results presented in Figure 5, we solved Equation 17 numerically using the "shooting method" (18) along with the additional relationships expressed by Equations 3 to 6 and with the parameters listed in Table V. The boundary conditions were:

$$p(R_{min}) = p_i \tag{19}$$

which sets CO_2 pressure equal to a desired p_i value at the

Table V. *Parameter Values Used in the Model to Generate Figure 5*

Parameter	Value	Units	Notes[a]
g^{b}_{liq}	$0.5 \times 0.9 \times W/Z$	μmol m^{-3} s^{-1} Pa^{-1}	1
K_a	1	Pa	2
K_m	71	Pa	2
R_{max}	$0.6769Z$	m	3
R_{min}	$0.05\ R_{max}$	m	4
$V_{c,max}$	$200/Z$	μmol m^{-3} s^{-1}	5
V_j	$20/Z$	μmol m^{-3} s^{-1}	5
W	15	—	6
Z	3×10^{-4}	—	—
α	0.3	μmol m^{-3} s^{-1}	2
β	2.5×10^{-3}	m^3 Pa μmol^{-1}	7
ϕ	0.25	—	8
Γ^*	4.2	Pa	2

[a] 1, Assumes 90% of mesophyll cell wall is lined with chloroplasts. Division by Z converts conductance to a volumetric basis; 2, Kirschbaum and Farquhar (8); 3, outer radius of hemispherical region. The constant scales the volume (see text); 4, inner radius of hemispherical region. This is the assumed radius of the substomatal cavity; 5, value as in ref. 24. Division by Z converts to a volumetric basis; 6, *cf.* Longstreth *et al.* (10); 7, conversion factor for units; and 8, assumed porosity (volumetric air space fraction) of mesophyll. [b] g_{liq}, volumetric liquid-phase conductance from cell wall to chloroplast; K_a, Michaelis-Menten constant for activation of ribulose-1,5-bisphosphate carboxylase/oxygenase (hereafter referred to in this footnote as Rubisco) by CO_2; K_m, effective Michaelis-Menten constant for CO_2, accounting for competitive inhibition by O_2; R_{max}, maximal radius; R_{min}, minimal radius; $V_{c,max}$, maximal local volumetric carboxylation rate when Rubisco is fully activated and when CO_2 and RuP_2 are not limiting; V_j, local volumetric potential carboxylation rate as limited by electron transport and photophosphorylation; W, cell-wall area per epidermal area; Z, typical thickness of mesophyll in a xerophyte; α, smoothing factor for the transition between Rubisco limitation and RuP_2 limitation; β, factor to match units between the diffusion rate to a point and the assimilation rate at that point; ϕ, local value of porosity (air-space fraction) over tortuosity; Γ^*, CO_2 compensation point.

boundary of the sub-stomatal cavity (which has radius R_{min}), and:

$$\frac{dp}{dr} = 0 \qquad \text{at} \qquad r = R_{max}, \tag{20}$$

where R_{max} is the outer radius of the equivalent hemispherical region served by one stoma. Equation 20 is equivalent to there being no diffusion out of the hemisphere at $r = R_{max}$. This region was chosen to have the same volume as would a hexagonal cylinder through the mesophyll with a stoma in the center of one end.

ACKNOWLEDGMENTS

We thank John Evans for the valuable suggestion to use helium for gas-exchange experiments, Graham Farquhar and Ian Cowan for help in developing the model, Rand Hooper for excellent technical assistance; and Gail Bingham for helpful technical advice. Farquhar, Evans, and two reviewers also provided helpful comments on drafts of the paper.

LITERATURE CITED

1. **Bykov OD, Levin ES** (1976) Internal and external processes of photosynthetic gas exchange in connection with CO_2 diffusion in the leaf. Soviet Plant Physiol **23:** 201–207
2. **Egorov VP, Karpushkin LT** (1988) Determination of air humidity over evaporating surface of a leaf by a compensation method. Photosynthetica **22:** 394–404
3. **Evans JR** (1983) Nitrogen and photosynthesis in the flag leaf of wheat (*Triticum aestivum* L.). Plant Physiol **72:** 297–302
4. **Evans JR, Terashima I** (1988) Photosynthetic characteristics of spinach leaves grown with different nitrogen treatments. Plant Cell Physiol **29:** 157–165
5. **Gutschick VP** (1984) Photosynthesis model for C3 leaves incorporating CO_2 transport, propagation of radiation, and biochemistry 1. Kinetics and their parameterization. Photosynthetica **4:** 549–568
6. **Jarvis PG** (1971) The estimation of resistances to carbon dioxide transfer. *In* Šesták, J Čatský, PG Jarvis, eds, Plant Photosynthetic Production, Manual of Methods. Dr. W. Junk N.V. Publishers, The Hague, pp 566–631
7. **Jones HG, Slatyer RO** (1972) Effects of intercellular resistances on estimates of the intracellular resistance to CO_2 uptake by plant leaves. Aust J Biol Sci **25:** 443–453
8. **Kirschbaum MUF, Farquhar GD** (1984) Temperature dependence of whole-leaf photosynthesis in *Eucalyptus pauciflora* Sieb. ex Spreng. Aust. J Plant Physiol **11:** 519–538
9. **Leunig, R** (1983) Transport of gases into leaves. Plant Cell Environ **6:** 181–194
10. **Longstreth DJ, Hartsock TL, Nobel PS** (1980) Mesophyll cell properties for some C3 and C4 species with high photosynthesis rates. Physiol Plant **48:** 494–498
11. **Mason EA, Marrero TR** (1970) The diffusion of atoms and molecules. Adv Atomic Mol Phys **6:** 155–232
12. **Mott KA, Gibson AC, O'Leary JW** (1982) The adaptive significance of amphistomatic leaves. Plant Cell Environ **5:** 455–460
13. **Parkhurst DF** (1977) A three-dimensional model for CO_2 uptake by continuously distributed mesophyll in leaves. J Theoret Biol **67:** 471–488
14. **Parkhurst DF** (1978) The adaptive significance of stomatal occurrence on one or both sides of leaves. J Ecol **66:** 367–383
15. **Parkhurst DF** (1986) Internal leaf structure: a three-dimensional perspective. *In* T Givnish, ed, On the Economy of Plant Form and Function. Cambridge University Press, New York, pp 215–249
16. **Parkhurst DF** (1987) Photosynthesis in relation to internal leaf structure (abstract). *In* Proceedings of the 14th International Botanical Congress, West Berlin, Federal Republic of Germany, p 383
17. **Parkhurst DF, Wong SC, Farquhar GD, Cowan IR** (1986) Gradients of intercellular CO_2 levels across the leaf mesophyll. Plant Physiol **86:** 1032–1037
18. **Press WH, Flannery BP, Teukolsky SA, Vetterling WT** (1989) Numerical Recipes in Pascal, Cambridge University Press, New York
19. **Rand RH** (1977) Gaseous diffusion in the leaf interior. Trans ASAE **20:** 701–704
20. **Rand RH, Cooke JR** (1980) A comprehensive model for CO_2 assimilation in leaves. Trans ASAE **23:** 601–607
21. **Rosenmann M, Morrison P** (1974) Maximum oxygen consumption and heat loss facilitation in small homeotherms by He-O_2. Am J Physiol **226:** 490–495
22. **Terashima I, Inoue Y** (1985) Vertical gradient in photosynthetic properties of spinach chloroplasts dependent on intra-leaf light environment. Plant Cell Phys **4:** 781–785
23. **Terashima I, Saeki T** (1985) A new model for leaf photosynthesis incorporating the gradients of light environment and of photosynthetic properties of chloroplasts within the leaf. Ann Bot **56:** 489–499
24. **von Caemmerer S, Farquhar GD** (1981) Some relationships between the biochemistry of photosynthesis and the gas exchange of leaves. Planta **153:** 376–387
25. **Wonnacott RJ, Wonnacott TH** (1985) Introductory Statistics, Ed 4, John Wiley & Sons, New York